MODELING THE PROGRESSIVE DAMAGE OF ADHESIVELY BONDED JOINTS

Anastasios P. Vassilopoulos, Roohollah Sarfaraz, Moslem Shahverdi, Thomas Keller

Composite Construction Laboratory (CCLab),
Ecole Polytechnique Fédérale de Lausanne, (EPFL),
Station 16, Bâtiment BP, CH-1015 Lausanne, Switzerland

Keywords: Polymer-matrix composites (PMCs); Fracture; Numerical analysis; Pultrusion.

Abstract

A quasi-static progressive damage model based on the fracture mechanics approach was developed for adhesively-bonded pultruded glass fiber-reinforced polymer (GFRP) joints. The model comprises the implementation in a numerical algorithm of a mixed-mode fracture failure criterion, experimentally developed using data acquired under pure Mode I and II and mixed-Mode I/II loading conditions. The bridging effect, as exhibited mainly by the R-curve behavior of the examined joints, was taken into account in the failure criterion. The numerical algorithm, assisted by finite element analysis for calculation of the strain energy release rate, was successfully employed for predicting the strength and the R-curve response of adhesively-bonded double-lap structural joints.

1. Introduction

Progressive damage modeling is a failure analysis technique that is widely used to predict the fracture behavior and strength of bonded joints based on the evolution of the damage state. Finite element analyses usually supplement numerical simulations of this type. Several approaches, such as the stress/strain approach, fracture mechanics, continuum mechanics, and cohesive zone modeling, have been introduced over recent decades for simulation of the damage progression in bonded joints under quasi-static loading.

The fracture mechanics approach, used to predict the static behavior of bonded joints is based on the fracture mechanics theory, see e.g. [1-2] for works based on the calculation of the critical stress intensity factor (SIF) or references [3-6] for works based on the critical strain energy release rate (G_c). In composite materials, the strain energy release rate (G) is usually preferred to stress intensity [7]. The main difficulty of using failure criteria based on the strain energy release rate is how to take into account the inherent fracture mode-mixity (interaction of fracture Modes I, II, and III) in structural joints. Several criteria have been introduced to model the interaction of Mode I and Mode II fracture energy, e.g. linear or quadratic criteria, however their modeling accuracy depends on the material system [4]. The determination of G and partition of different fracture modes are also essential steps in fracture mechanics, especially when the crack propagates along a bi-material interface. The most popular method based on linear elastic fracture mechanics (LEFM) to calculate the G using numerical models, able to partition the components of G, is the virtual crack closure technique (VCCT) [8]. The main disadvantage of the VCCT is the self-similar crack propagation requirement. This necessitates a moving mesh that must be refined around the crack tip and limits the

propagation to a straight crack path; e.g. in layered composite materials, for a crack initiated between two layers, it must propagate between the same layers [9-10]. Also, an initial crack must be introduced in the finite element model, making this approach inappropriate for prediction of the crack initiation phase [5, 9, 10].
The fracture mechanics approach is appropriate for adhesively-bonded GFRP joints with geometrical discontinuities that provoke stress singularities. In such cases crack propagation is self-similar since the propagation path usually remains between the adherends bonded with the adhesive or in between two layers of adherends [11-12]. In addition, the model parameters can be directly deduced from experiments and with the rapid improvement in computational resources over recent years, the problem of mesh refinement around the crack tip is no longer a major issue. However, the studies performed on this topic were mainly focused on the cohesive failure mode [6] while in FRP bonded joints fiber-tear failure of composite adherends has also been observed accompanied by fiber bridging. A previous study by the present authors, on pultruded GFRP joints showed a significant contribution (as high as 60%) of fiber bridging in the total strain energy release rate, [13]. However, the bridging effect was ignored in existing models e.g. [5] for the sake of simplicity.
A progressive damage model for adhesively-bonded pultruded GFRP structural joints under quasi-static loading, taking fiber bridging into account, is presented in this work. A numerical algorithm was developed with the model parameters estimated according to fracture mechanics data from double cantilever beam (DCB), end-loaded-split (ELS), and mixed-mode bending (MMB) experiments. A mixed-mode fracture criterion, taking into account the fiber-bridging effect established in a previous work [13], was employed in this algorithm. The good agreement between prediction of the quasi-static behavior of the examined structural joints and experimental data demonstrated the suitability and accuracy of the method.

2. Experimental investigation

2.1. Materials

Adhesively-bonded joints composed of pultruded GFRP laminates bonded by an epoxy adhesive system were examined under pure Mode I and II and four different mixed-Mode I/II loading conditions. The pultruded GFRP laminates, supplied by Fiberline A/S, Denmark, consisted of E-glass fibers and isophthalic polyester resin. The laminates comprised two mat layers on each side and a roving layer in the middle with a thin layer of polyester veil on the outer surfaces. Each mat layer comprised of 0/90 woven fabric stitched to a chopped strand mat (CSM). The GFRP laminates showed a linear elastic behavior up to failure with the average longitudinal strength and Young's modulus of 307 MPa and 25 GPa respectively under tensile experiments. A two-component epoxy adhesive system was used (Sikadur 330, Sika AG, Switzerland) as the bonding material. The epoxy showed an almost elastic behavior and a brittle failure under quasi-static tensile loading [14].

2.2. Joint geometry and fabrication

Schematic figures of the asymmetric DCB, ELS and MMB specimens used in this study are shown in Figs. 1-2. The specimen lengths were 250 mm for DCB and 400 mm for ELS, and MMB specimens respectively. The free length of the ELS specimen was 300 mm and the half-span length for the MMB was 170 mm. A Teflon film of 0.05-mm thickness was placed between one of the laminates and the adhesive layer to introduce the pre-crack of 50, 140, and 50 mm, measured from the loading line, respectively for DCB, ELS, and MMB [11]. The

resulting fracture mechanics joints were asymmetric since the pre-crack was placed away from the mid-plane. Symmetric double-lap joints, without pre-crack, composed of the same materials with the total length of 410 mm were also fabricated, see Fig. 3. [12].

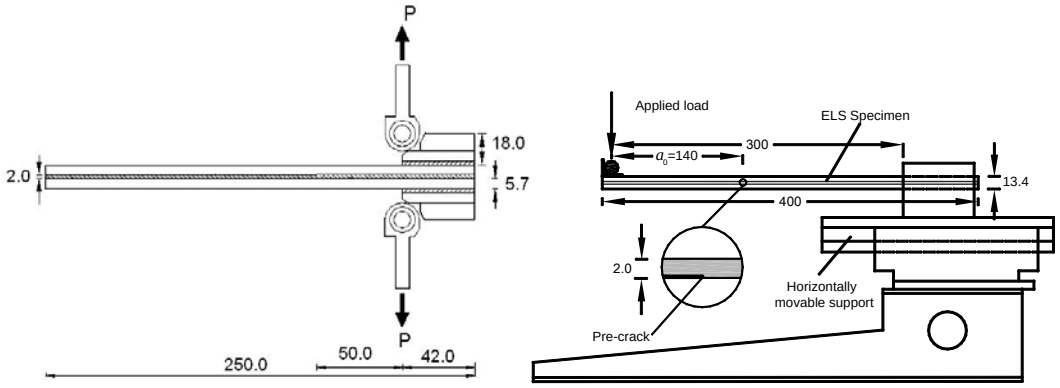

Figure 1. DCB and ELS specimen configuration, dimensions in [mm]

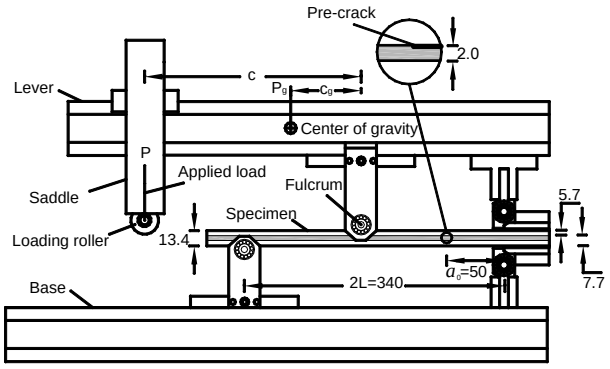

Figure 2. Schematic of mixed mode bending apparatus, dimensions in [mm]

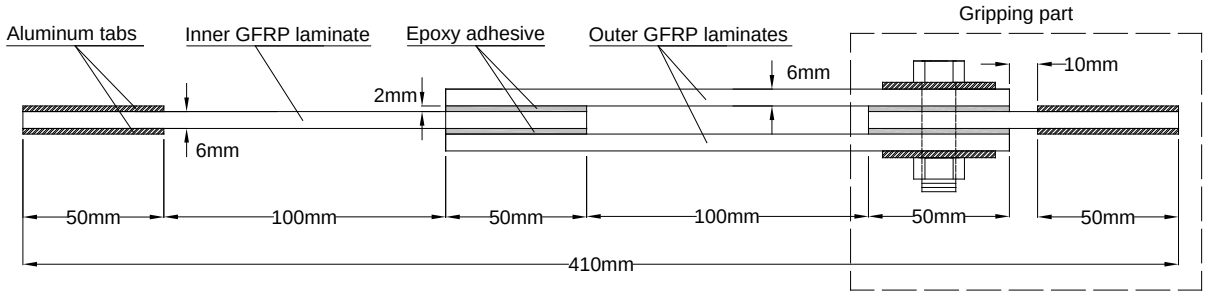

Figure 3. Double-lap joint geometry

2.3. Experimental program and set-up

The DCB fracture experiments were performed on a testing machine of 5-kN capacity, under displacement control at a constant rate of 1 mm/min, according to ASTM5528-01(2007).A 25-kN MTS Landmark servo-hydraulic testing rig, calibrated to 20% of its maximum capacity, was employed for loading the ELS and MMB experiments. Both types of specimens were loaded under displacement control at a constant rate of 1 mm/min. The crack length in these experiments was determined by means of a video extensometer. In the MMB experimental set-up, the load was applied at the lever at distance c from the fulcrum. The length of the loading lever determined the mode ratio for the experiment. The right end of the specimen was loaded using in-house developed piano hinges. The applied loads and

displacements were continuously recorded. The MMB experiments were performed under four different lever lengths, c=227, 150, 100, and 60 mm, corresponding to the nominal G_I/G_{II} equal to 3.70, 2.20, 1.08, and 0.28 respectively [15]. Quasi-static tensile experiments on the DLJ specimens were carried out on an INSTRON 8800 servo-hydraulic machine of 100-kN capacity under displacement-control mode at under 1 mm/min. One specimen was instrumented on both sides by two crack gages to monitor crack initiation and propagation during the experiment [12].
All experiments were conducted under laboratory conditions, i.e. 23±5 °C and 50±10% RH. The experimental results obtained from a total of 8 DCB [11], 9 ELS [13], 21 MMB [15], and 5 DLJ [12] specimens were used to establish and validate the progressive damage model. The fracture mechanics joints, i.e. DCB, ELS, and MMB specimens, were employed for developing the fracture failure criterion and establishing the model and the DLJs were used for the evaluation the process.

2.4. Load-displacement response and R-curve behavior

Linear load-displacement responses were observed up to crack initiation in all cases. The load increased up to the maximum value and then gradually decreased, although for the ELS specimen the load decrement was not as significant, as shown in Fig. 4(a) for a DCB specimen.
The strain energy release rate of the examined joints was also calculated based on the LEFM theory as the behavior of the constituent materials is linear elastic up to failure. The strain energy release rate calculation and fracture mode partition for MMB specimens were carried out based on the extended global method presented in [15].
The total strain energy release rate can be expressed as the sum of the energy release rate at the crack tip, G_{tip}, and the energy release rate due to fiber bridging, G_{br}, components i.e. $G=G_{tip}+G_{br}$. Generally, the strain energy release rate (G) of composite materials gradually increases due to the fiber bridging until it reaches a plateau (R-curve). This curve describes the relationship between the crack length and the corresponding G [11]. Indicative R-curve for the DCB joints is illustrated in Fig. 4(b).

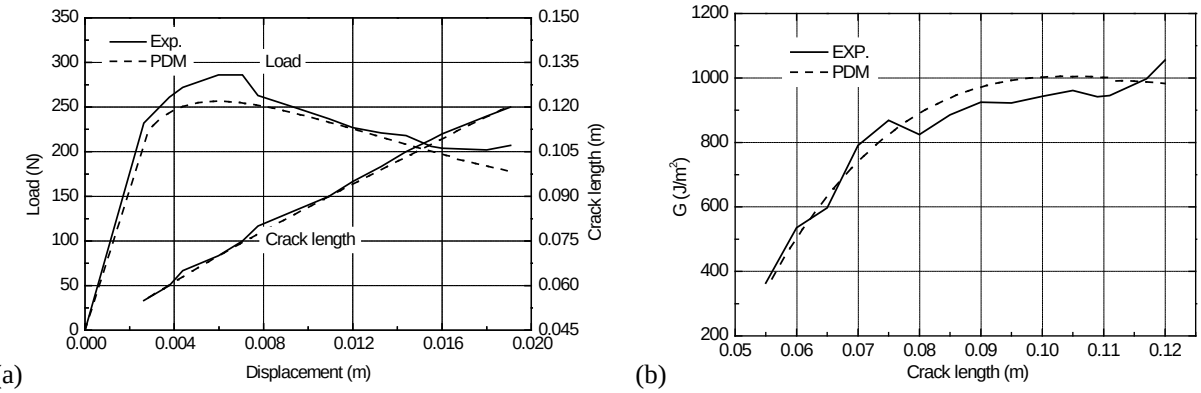

Figure 4. Comparison of load-displacement response from experimental investigation and FE model (a) and of R-curve response from experimental investigation and FE model for DCB specimen (b).

The mean value of the visually determined plateau - taking the typical scatter of this type of material into account - was assumed to represent the G for steady state propagation (G_{pro}). The initial value of the G (G_{ini}) was determined based on the observed nonlinearity of the load-displacement curves.

The six R-curves obtained under Mode I, Mode II, and four different mode-mixities exhibit a similar increasing trend until reaching a plateau. The R-curves were scaled to the range [0, 1] by adjusting the G_{ini} to 0 and the G_{pro} to 1 using the following relationship:

$$G_{scaled}(a) = \frac{G(a) - G_{ini}}{G_{pro} - G_{ini}} \tag{1}$$

The crack lengths required to reach the plateau, i.e. the fiber-bridging lengths [11], varied slightly between the different specimen types and the mode-mixity. Nevertheless there was no specific trend among the normalized R-curves with respect to mode-mixity. Therefore, as a similar failure mode was observed for all fracture mode configurations, an average of the normalized R-curves was considered as the master R-curve of the examined material system. This master R-curve can be expressed as follows:

$$R(a) = 3654a^3 - 730a^2 + 47a \tag{2}$$

3. Failure criterion

The results of the experimental investigations under different mode-mixities ranging from pure Mode I to pure Mode II allows the establishment of mixed-mode fracture failure criteria. The details of the experimental program and the data reduction procedure employed to establish such failure criteria for the examined material were discussed in [38]. For practical reasons, among the different ways of presenting the failure criterion, in this study it was preferred to plot the experimental results in terms of $G_{tot}=G_I+G_{II}$ versus G_{II}/G_{tot}, see Fig.5. As mentioned above both the energy release rate components corresponding to fiber bridging and the crack tip are considered. As can be observed in Fig. 5, the G_{tot} increased as the G_{II}/G_{tot} increased. A second order polynomial in the form of Eq. (3) expresses these criteria:

$$G_{tot} = A(\frac{G_{II}}{G_{tot}})^2 + B(\frac{G_{II}}{G_{tot}}) + C \tag{3}$$

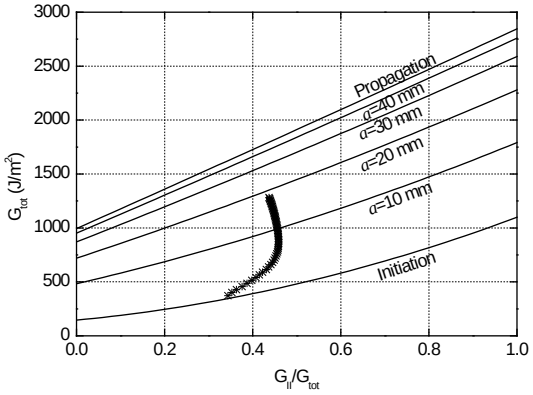

Figure 5. Mixed-mode failure criterion at different crack lengths

The master R-curve given in Eq. (3) can be used to estimate the mixed-mode strain energy release rate, taking into account fiber bridging, for any crack length as:

$$G_{tot}\left(a, \frac{G_{II}}{G_{tot}}\right) = A(a)(\frac{G_{II}}{G_{tot}})^2 + B(a)(\frac{G_{II}}{G_{tot}}) + C(a) \tag{4}$$

with parameters A(a), B(a), and C(a) determined by Eqs. (5)-(7) as functions of the master R-curve:

$$A(a) = R(a).\left(A_{pro} - A_{ini}\right) + A_{ini} \quad (5)$$

$$B(a) = R(a).\left(B_{pro} - B_{ini}\right) + B_{ini} \quad (6)$$

$$C(a) = R(a).\left(C_{pro} - C_{ini}\right) + C_{ini} \quad (7)$$

4. Progressive damage model

The virtual crack closure technique (VCCT) was used for calculation of the fracture parameters at the crack tip. Bi-material interfaces were present in all specimens with cracks propagating between the mat layers and therefore the obtained mode-mixity was sensitive to the Δa, and did not converge to any particular value when Δa approached infinitesimal values. In order to avoid this problem, a thin layer, designated the "resin interlayer", with the average properties of the adjacent layers of the interface was inserted at the interface [16]. The thickness of the resin interlayer was selected as being 0.1 mm as a compromise resulting in almost no changes in the stiffness of the model (less than 1%) and also introducing a reasonable number of elements into the FE models. The element size was selected to ensure there were at least two elements along the thickness of each layer. This constraint was imposed on the thin resin layer to satisfy the self-similarity condition required for VCCT and eliminated the sensitivity of the calculated mode-mixity to the element size as presented in [16].
The algorithm of the progressive damage modeling of bonded joints, programmed in ANSYS parametric design language (APDL), is shown in Fig. 6:

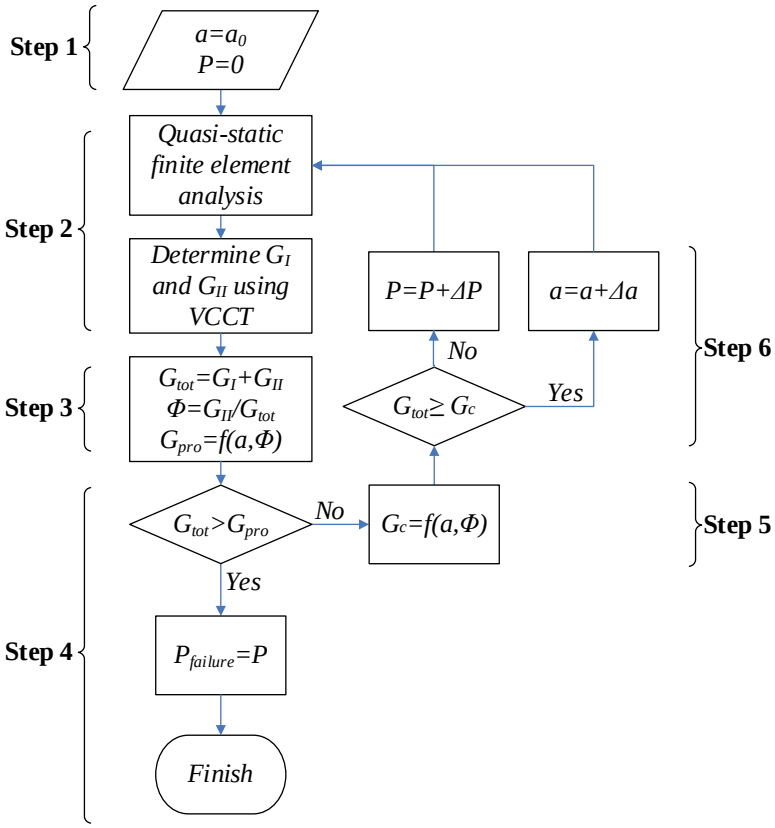

Figure 6. Flow chart of strength prediction method

5. Results and discussions

Prior to the application of the algorithm for prediction of the fracture behavior of a structural joint, the proposed numerical algorithm was validated by simulating the load-displacement and the R-curve behavior of the fracture mechanics joints. The load-displacement curves reproduced for DCB, ELS, and MMB specimens are corroborated very well by the experimental data (Exp.). The R-curves derived using the numerical algorithm also present good agreement with the experimental curves (see indicative result in Fig. 4(b)).
The changes in the fracture parameters (G_I, G_{II}, G_{tot}, and G_I/G_{II}) versus the crack length for a DLJ specimen were numerically derived (Step 2) under a constant load of 20 kN. Both G_I and G_{II} showed a monotonically increasing trend with increasing crack length; see Fig. 7(a). G_{II} increased more than G_I for short crack lengths of up to around 5 mm and then remained almost constant up to 25 mm and finally increased rapidly up to the end of the bonding length. The increase rate of G_I was low and almost constant up to the crack length 25 mm, corresponding to the half-length of the bond line, and then suddenly increased.

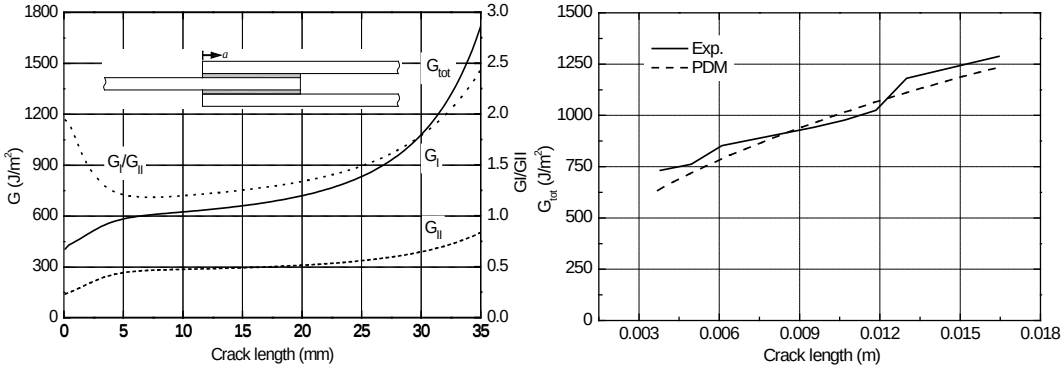

Figure 7. Variation of G_I, G_{II}, and G_{tot} vs. crack length for DLJ (a) and comparison of R-curve response from experimental investigation and PDM for DLJ specimen (b)

The quasi-static fracture behavior of the DLJ was predicted using the progressive damage model. The variation of G_{tot} versus G_{II}/G_{tot} as the crack grows between initiation and propagation is indicated in Fig. 5 by star symbols. The experimentally derived R-curve for the DLJ, presented in Fig. 7(b) is corroborated well by the predicted one using the progressive damage model, also presented in the same figure.

6. Conclusions

A progressive damage model based on the fracture mechanics approach is proposed for adhesively-bonded pultruded structural GFRP joints. A fracture failure criterion was established using experimental data from fracture mechanics joints. The prediction accuracy of the failure criterion was furthermore assessed by estimating the strength and reproducing the R-curve response of a typical adhesively-bonded double-lap joint system.
The fiber-bridging effects can be successfully taken into account by the fracture failure criterion, allowing accurate prediction of the R-curve behavior of the examined joints under mixed-mode fracture. The accurate prediction of the crack initiation, load-displacement curve, failure load, and R-curve behavior of the examined structural joints proved the applicability of the developed numerical algorithm to complex joint configurations.

Acknowledgements
This work was supported by the Swiss National Science Foundation (Grant No 200020-121756), Fiberline Composites A/S, Denmark (supplier of the pultruded laminates), and Sika AG, Zurich (adhesive supplier).

References

[1] Groth HL, Stress singularities and fracture at interface corners in bonded joints, *Int J Adhes Adhes*, 1988;8(2):107-113.
[2] Gleich DM, Van Tooren MJL, Beukers A. A stress singularity approach to failure initiation in a bonded joint with varying bondline thickness, *J Adhes Sci Technol*, 2001;15(10):1247-1259.
[3] Johnson WS, Mall S. A fracture mechanics approach for designing adhesively-bonded joints, delamination and debonding of materials, ASTM, STP876, Johnson WS Ed. Philadelphia, 1985, pp. 189-199.
[4] Tong L. Strength of adhesively-bonded single-lap and lap-shear joints, *Int J Solids Struct*, 1998;35(20):2601-2616.
[5] Hoyt DM, Ward SH, Minguet PJ. Strength and fatigue life modeling of bonded joints in composite structure. *J Compos Tech Res*, 2002;24(3):188-208.
[6] Azari S, Eskandarian M, Papini M, Schroeder JA, Spelt JK. Fracture load predictions and measurements for highly toughened epoxy adhesive joints, *Eng Fract Mech*, 2009;76(13):2039-2055.
[7] Kinloch AJ (1987), Adhesion and adhesives: science and technology, Chapman & Hall, London.
[8] Rybicki EF, Kanninen MF. A finite element calculation of stress intensity factors by a modified crack closure integral, *Eng Fract Mech*, 1977;9(4):931-938.
[9] Fan XL, Sun Q, Kikuchi M, Review of damage tolerant analysis of laminated composites, *J solid mech*, 2010;2(3):275-289.
[10] Tay TE, Liu G, Tan VBC, Sun XS, Pham DC. Progressive failure analysis of composites, *J Compos Mater*, 2008;42(18):1921–1966.
[11] Shahverdi M, Vassilopoulos AP, Keller T. A phenomenological analysis of Mode I fracture of adhesively-bonded pultruded GFRP joints. *Eng Fract Mech*, 2011;78(10):2161-2173.
[12] Sarfaraz R, Vassilopoulos AP, Keller T. Experimental investigation of the fatigue behavior of adhesively-bonded pultruded GFRP joints under different load ratios. *Int J Fatigue*, 2011;33(11):1451–60.
[13] Shahverdi M, Vassilopoulos AP, Keller T. Mixed-mode quasi-static failure criteria for adhesively-bonded pultruded GFRP joints Failure. *Compos Part A – Appl Sci*, 2014;59:45-56.
[14] De Castro J, Keller T. Ductile double-lap joints from brittle GFRP laminates and ductile adhesives. Part I: experimental investigation. *Compos Part B – Eng*, 2008;39(2):271–281.
[15] Shahverdi M, Vassilopoulos AP, Keller T. Mixed-Mode I/II fracture behavior of asymmetric adhesively-bonded pultruded composite joints. *Eng Fract Mech*, 2014;115:43-59.
[16] Shahverdi M, Vassilopoulos AP, Keller T. Modeling effects of asymmetry and fiber bridging on Mode I fracture behavior of bonded pultruded composite joints. *Eng Fract Mech*, 2013; 99:335-348.